AMERICAN SOCIETY FOR MICROBIOLOGY | Journal of Virology®

PRIONS

Melanin or a Melanin-Like Substance Interacts with the N-Terminal Portion of Prion Protein and Inhibits Abnormal Prion Protein Formation in Prion-Infected Cells

Taichi Hamanaka,[a] Keiko Nishizawa,[a] Yuji Sakasegawa,[a] Ayumi Oguma,[a] Kenta Teruya,[a] Hiroshi Kurahashi,[a]* Hideyuki Hara,[b] Suehiro Sakaguchi,[b] Katsumi Doh-ura[a]

Department of Neurochemistry, Tohoku University Graduate School of Medicine, Sendai, Japan[a]; Division of Molecular Neurobiology, Institute for Enzyme Research, Tokushima University, Tokushima, Japan[b]

ABSTRACT Prion diseases are progressive fatal neurodegenerative illnesses caused by the accumulation of transmissible abnormal prion protein (PrP). To find treatments for prion diseases, we searched for substances from natural resources that inhibit abnormal PrP formation in prion-infected cells. We found that high-molecular-weight components from insect cuticle extracts reduced abnormal PrP levels. The chemical nature of these components was consistent with that of melanin. In fact, synthetic melanin produced from tyrosine or 3-hydroxy-L-tyrosine inhibited abnormal PrP formation. Melanin did not modify cellular or cell surface PrP levels, nor did it modify lipid raft or cellular cholesterol levels. Neither did it enhance autophagy or lysosomal function. Melanin was capable of interacting with PrP at two N-terminal domains. Specifically, it strongly interacted with the PrP region of amino acids 23 to 50 including a positively charged amino acid cluster and weakly interacted with the PrP octarepeat peptide region of residues 51 to 90. However, the *in vitro* and *in vivo* data were inconsistent with those of prion-infected cells. Abnormal PrP formation in protein misfolding cyclic amplification was not inhibited by melanin. Survival after prion infection was not significantly altered in albino mice or exogenously melanin-injected mice compared with that of control mice. These data suggest that melanin, a main determinant of skin color, is not likely to modify prion disease pathogenesis, even though racial differences in the incidence of human prion diseases have been reported. Thus, the findings identify an interaction between melanin and the N terminus of PrP, but the pathophysiological roles of the PrP-melanin interaction remain unclear.

IMPORTANCE The N-terminal region of PrP is reportedly important for neuroprotection, neurotoxicity, and abnormal PrP formation, as this region is bound by many factors, such as metal ions, lipids, nucleic acids, antiprion compounds, and several proteins, including abnormal PrP in prion disease and the Aβ oligomer in Alzheimer's disease. In the present study, melanin, a main determinant of skin color, was newly found to interact with this N-terminal region and inhibits abnormal PrP formation in prion-infected cells. However, the data for prion infection in mice lacking melanin production suggest that melanin is not associated with the prion disease mechanism, although the incidence of prion disease is reportedly much higher in white people than in black people. Thus, the roles of the PrP-melanin interaction remain to be further elucidated, but melanin might be a useful competitive tool for evaluating the functions of other ligands at the N-terminal region.

KEYWORDS drug discovery, mechanisms of action, melanin, prions

Received 14 September 2016 **Accepted** 5 January 2017

Accepted manuscript posted online 11 January 2017

Citation Hamanaka T, Nishizawa K, Sakasegawa Y, Oguma A, Teruya K, Kurahashi H, Hara H, Sakaguchi S, Doh-ura K. 2017. Melanin or a melanin-like substance interacts with the N-terminal portion of prion protein and inhibits abnormal prion protein formation in prion-infected cells. J Virol 91:e01862-16. https://doi.org/10.1128/JVI.01862-16.

Editor Byron Caughey, Rocky Mountain Laboratories

Address correspondence to Katsumi Doh-ura, doh-ura@med.tohoku.ac.jp.

* Present address: Hiroshi Kurahashi, Laboratory for Protein Conformation Diseases, RIKEN Brain Science Institute, Wako, Japan.

T.H. and K.N. contributed equally to this work.

Prion diseases, also called transmissible spongiform encephalopathies, are progressive fatal neurodegenerative illnesses that include Creutzfeldt-Jakob disease in humans and scrapie, bovine spongiform encephalopathy, and chronic wasting disease in animals. These diseases are characterized by the accumulation in the brain of abnormal prion protein (PrP), which is a main component of pathogens that is conformationally converted from normal PrP (PrPc) (1). Abnormal PrP forms an insoluble protein polymer with a protease-resistant core (PrPres). The conversion of PrPc to abnormal PrP is a key event in prion formation of prion diseases.

Regarding treatments for these diseases, dozens of compounds or substances have been reported to either inhibit prion formation in prion-infected culture cells or prolong incubation periods in prion-infected animals (2–4). Some of these agents have been used in clinical trials against human prion diseases, but sufficiently beneficial effects in patients have never been reported (5–10). In humans, most cases of prion diseases sporadically occur mainly in elderly people, and obvious racial differences exist in the incidence of the diseases. Surveillance of prion diseases in the United States revealed that the age-adjusted incidence for white people is 2.7-fold higher than that for black people (11). However, the genetic and nongenetic factors responsible for disease susceptibility are largely unknown (12). These factors were similarly unveiled in acquired forms of prion disease such as variant Creutzfeldt-Jakob disease, which occurs unevenly in young people despite similar risks for prion infection (13).

To help in drug development for prion diseases, we searched for compounds or substances that modify abnormal PrP formation in prion-infected cells. In earlier reports (14, 15), medicinal compounds or natural products approved by the U.S. Food and Drug Administration were extensively screened for antiprion activities, and thus, we focused on the untouched materials of natural resources. In fact, we previously reported antiprion substances extracted from natural products such as fucoidan (16) and protein-bound polysaccharide K (17). The insect represents an undercultivated natural resource that exists abundantly in both number and variety, and there is a possibility to identify new insect-derived substances useful for either probing the PrP conversion mechanism or developing therapeutic or prophylactic drugs for prion diseases. In fact, anticancer, antiviral, or antimicrobial compounds are present in extracts from insects (18–21). In this study, we report antiprion substances derived from insects that have not been previously reported. The nature of the substances implicated that the antiprion components are melanin-like. Thus, the antiprion action of melanin was further studied in the present study, and we discuss the potential relevance of the findings.

RESULTS

Antiprion activities of insect extracts. Nine samples obtained from seven different insect species via extraction with sodium hydroxide and autoclaving were examined in neuroblastoma cells persistently infected with prion strain RML (ScN2a cells). All samples were black or dark brown solutions. Cells were incubated with 0.5% (vol/vol) insect extract samples equivalent to 0.5 mg of the initial materials per milliliter of culture medium for 3 days. Then, PrPres was assayed by immunoblotting. Consequently, all samples (Fig. 1A) except one extract sample (lane 4) significantly inhibited abnormal PrP formation. In particular, samples from adults of *Chalcosoma chiron* (Caucasus beetle), the larval shell of *Graptopsaltria nigrofuscata* (large brown cicada), and adults of *Allomyrina dichotoma* (Japanese horned beetle) had more-potent activities (Fig. 1A, lanes 1, 2, and 6, respectively).

We focused on two samples, and those from *C. chiron* and *A. dichotoma* were further examined in three distinct prion strain-infected cells. Both samples displayed antiprion activities in all three cell cultures (Fig. 1B). Although PrPc expression levels in N167 and F3 cells are typically 5-fold that in ScN2a cells (22, 23), antiprion activities of these samples appeared to be similarly potent in ScN2a and N167 cells but less potent in F3 cells, based on the 50% effective concentration value (EC_{50}) of each sample. These data suggest that both samples exert antiprion activities in a prion strain-dependent man-

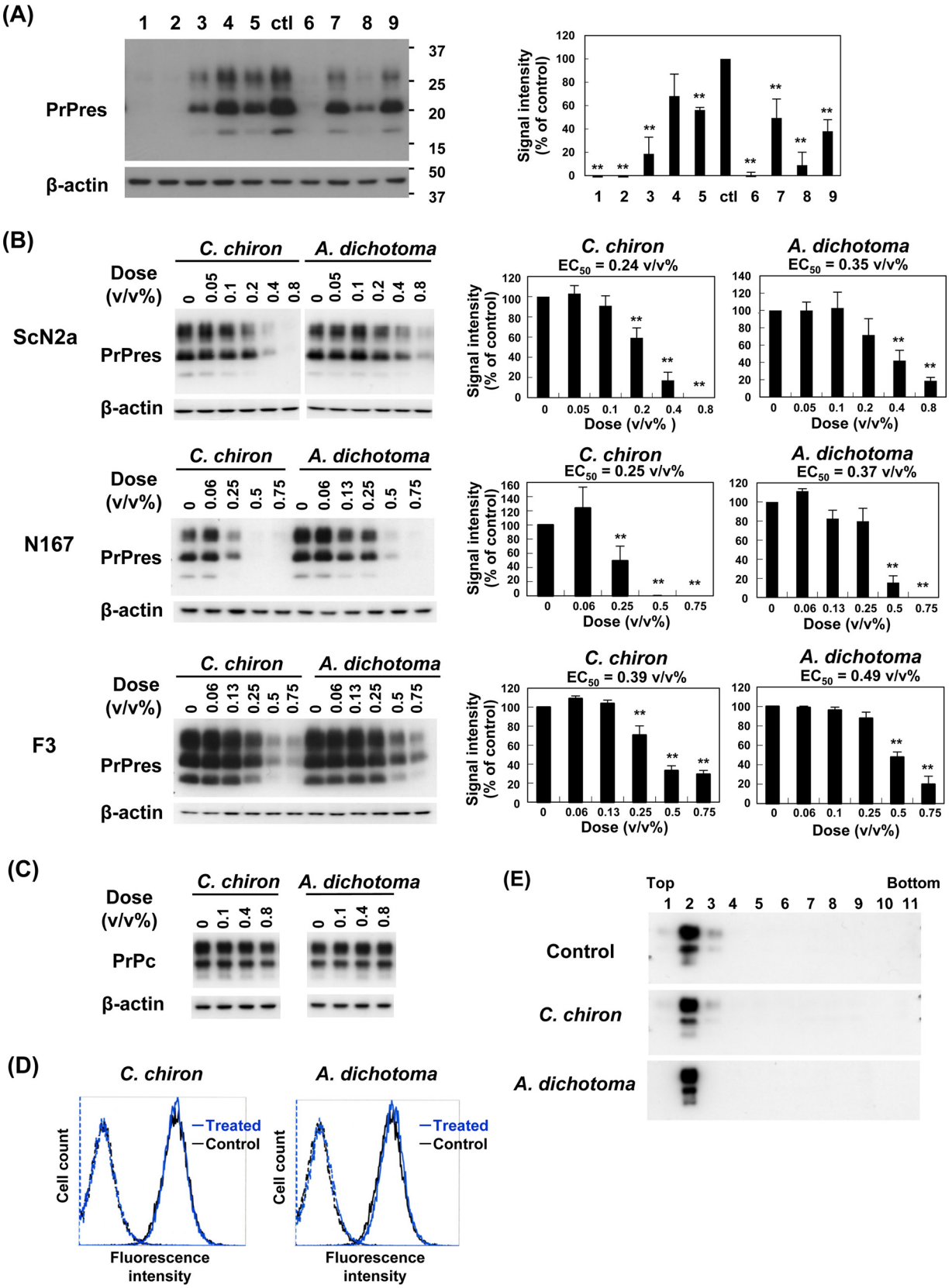

FIG 1 Antiprion activities of insect extracts. (A) Immunoblot data for PrPres in ScN2a cells treated with each insect extract. Lanes 1 to 9 correspond to the extracts from the adult body of *Chalcosoma chiron*, the larval shell of *Graptopsaltria nigrofuscata*, the adult body of *Halyomorpha halys*, the adult body of *Agrus convolvuli*, the adult body of *Papilio protenor*, the adult body of *Allomyrina dichotoma*, the adult body of *Graptopsaltria nigrofuscata*, the larval head of *Dorcus hopei binodulosus*, and the remaining parts of the larva of *Dorcus hopei binodulosus*, respectively. Cells were

(Continued on next page)

ner; the prion strain in F3 cells is likely to be less sensitive to both samples than the other two prion strains.

These samples did not modify PrPc (Fig. 1C) or cell surface PrPc levels in N2a cells (Fig. 1D). Compounds such as cholesterol modulators disturb the lipid raft microdomain of the cell membrane, a possible site of PrP conversion or interaction between PrPc and abnormal PrP (24–35). However, these samples did not modify PrPc localization in the flotation assay fractions for detergent-insoluble lipid raft membrane complexes in N2a cells (Fig. 1E). These data imply that the samples exert antiprion activities without modifying PrPc turnover or metabolism.

Characterization of insect extracts. Using the sample of *C. chiron* as a representative, the antiprion components of the insect extract were characterized. Ultrafiltration of membranes with four different pore sizes illustrated that the antiprion activity was predominantly localized in a fraction larger than 100 kDa (Fig. 2A). Because cuticles are predominantly included in insects, we examined whether high-molecular-weight components of cuticles such as chitin, β-glucan, protein, and melanin are linked to the antiprion activity. We treated the *C. chiron* sample with chitinase, zymolyase, and proteinase K to enzymatically digest chitin, β-glucan, and protein, respectively. Subsequently, these treatments did not modify the antiprion activity of the sample (Fig. 2B). We further examined the possibility of chitin involvement in the antiprion activity by using the water-soluble chitin derivative hydroxypropyl chitin, but it was apparently ineffective in inhibiting abnormal PrP formation (Fig. 2C).

Conversely, treatment with NaClO bleached the *C. chiron* sample and simultaneously abolished its antiprion activity (Fig. 2D). In addition, cation exchange chromatography revealed that antiprion components of the *C. chiron* sample were not bound to sulfopropyl ion exchange resin (Fig. 2E), suggesting that the antiprion components are negatively charged. Because melanin is known to be a naturally occurring cation exchange material (36), all of the data suggest that melanin or a melanin-like substance, especially eumelanin (see its representative structural formula in Fig. 2F), which is the most common type observed in black and brown-colored biological substances, is implicated in the antiprion activity.

Antiprion activities of synthetic melanin compounds. To test this implication, we assayed two types of synthetic melanin, namely, commercially available melanin that had been prepared via the oxidation of tyrosine (tyr-melanin) and melanin that we prepared from 3-hydroxy-L-tyrosine (dopa-melanin). Both synthetic compounds inhibited abnormal PrP formation in all three prion-infected cell cultures (Fig. 3A). These compounds were similar to the samples of *C. chiron* and *A. dichotoma* in terms of both being least potent in F3 cells; however, these compounds were obviously more potent than the insect samples in ScN2a cells (Fig. 3A). Neither compound modified PrPc levels in N2a cells (Fig. 3B), nor did either modify cell surface PrPc or cholera toxin B-binding lipid raft levels in N2a cells (Fig. 3C). The compounds also did not modify PrPc localization in the flotation assay fractions for detergent-insoluble lipid raft membrane complexes in N2a cells (Fig. 3D). In addition, cholesterol levels were not changed in N2a cells treated with either compound (Fig. 3E), and internalization of cell surface PrPc was not modified in N2a cells treated with a melanin compound (Fig. 3F). These data

FIG 1 Legend (Continued)
treated with 0.5% insect extracts, which were equivalent to 0.5 mg of the initial insect materials per milliliter of culture medium. Signals for β-actin are shown as controls for the integrity of samples used for PrPres detection. PrP signals were detected with the anti-PrP monoclonal antibody SAF83 in this analysis and the following analyses, unless otherwise specified. Molecular size markers on the right indicate sizes in kilodaltons. The bar graph shows averages and standard deviations for triplicate experiments (**, $P < 0.01$). Samples in lanes 1 and 6 were used for subsequent analyses. (B) Immunoblot data for PrPres in three distinct prion strain-infected cell lines treated with two representative insect extracts from *C. chiron* and *A. dichotoma*. The bar graph shows averages and standard deviations for triplicate experiments (**, $P < 0.01$). The 50% effective concentration value (EC_{50}) of each extract is also shown. (C) Immunoblot data for PrPc in N2a cells treated with extracts from *C. chiron* and *A. dichotoma*. (D) Flow cytometry of cell surface PrPc in N2a cells treated with 0.5% (vol/vol) extracts from *C. chiron* and *A. dichotoma*. Blue and black lines indicate insect extract-treated and untreated cells, respectively. The broken-line peaks on the left show their respective isotype controls. (E) Immunoblot data of PrPc fractionated by the flotation assay in N2a cells treated with 0.5% (vol/vol) extracts from *C. chiron* and *A. dichotoma*. The fraction numbers are indicated from the top to the bottom.

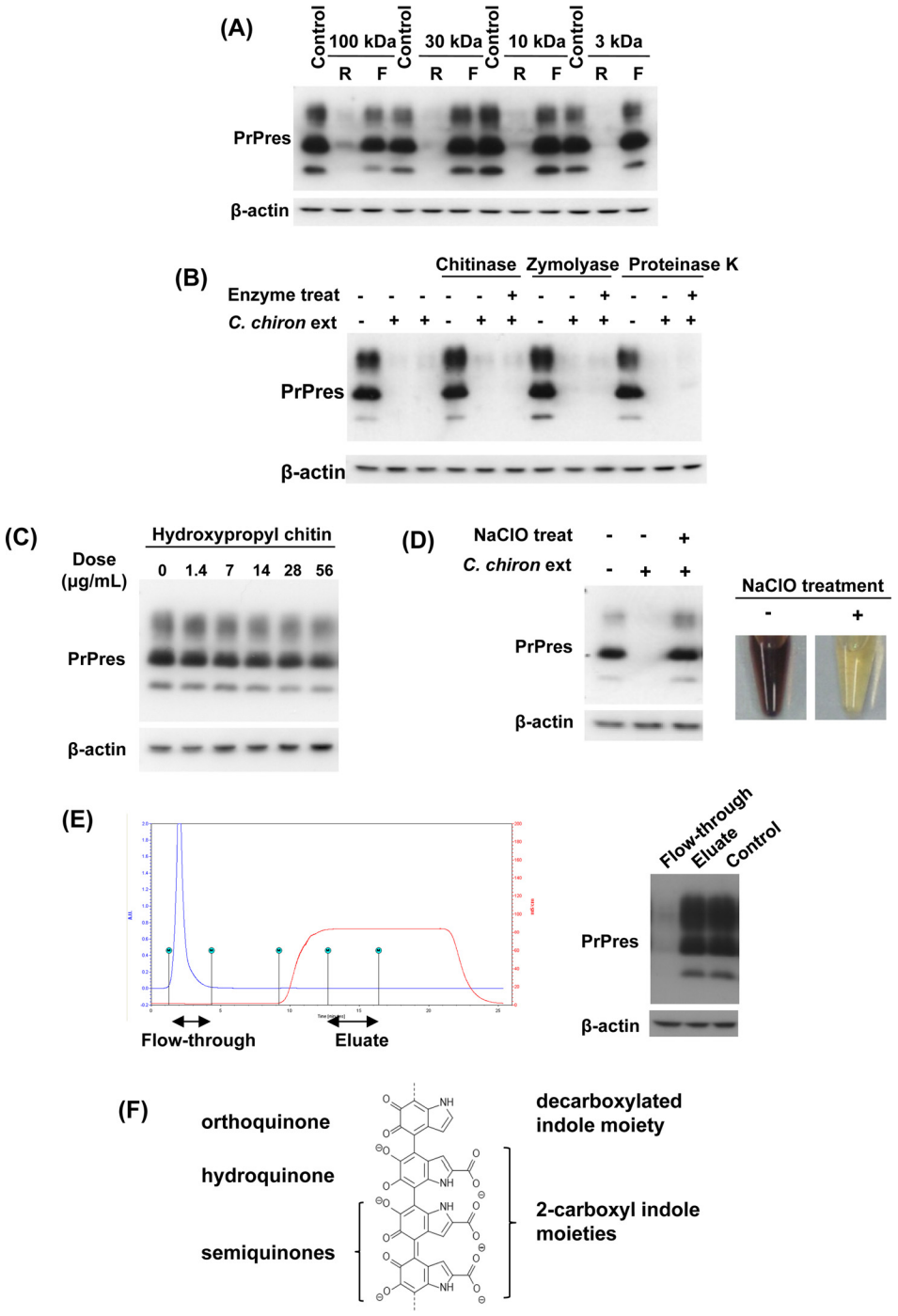

FIG 2 Characterization of insect extracts. (A) Immunoblot data for PrPres in ScN2a cells treated with the retentate (R) or filtrate (F) of 0.5% (vol/vol) *C. chiron* extract ultrafiltrated with membranes of designated molecular mass cutoff values. (B) Immunoblot data for PrPres in ScN2a cells treated with enzymatically digested 0.5% (vol/vol) *C. chiron* extract. (C) Immunoblot data for PrPres in ScN2a cells treated with water-soluble hydroxypropyl chitin. (D) Immunoblot data for PrPres in ScN2a cells treated with 0.5% (vol/vol) *C. chiron* extract that had been decomposed and decolored using NaClO. (E) Cation exchange chromatogram of *C. chiron* extract and immunoblot data of PrPres in ScN2a cells treated with the flowthrough or eluate. (F) Part of the structural formula of the most common type of melanin, eumelanin. Eumelanin is a representative black- or brown-colored biological pigment and is a conjugated polymer of orthoquinone, hydroquinone, and semiquinones.

suggest that synthetic melanin compounds exert antiprion activities without modifying PrPc turnover or metabolism, as previously observed for insect extract samples.

Characterization of melanin antiprion activities. Our examination found that the molecular sizes of antiprion activities in synthetic melanin compounds were also

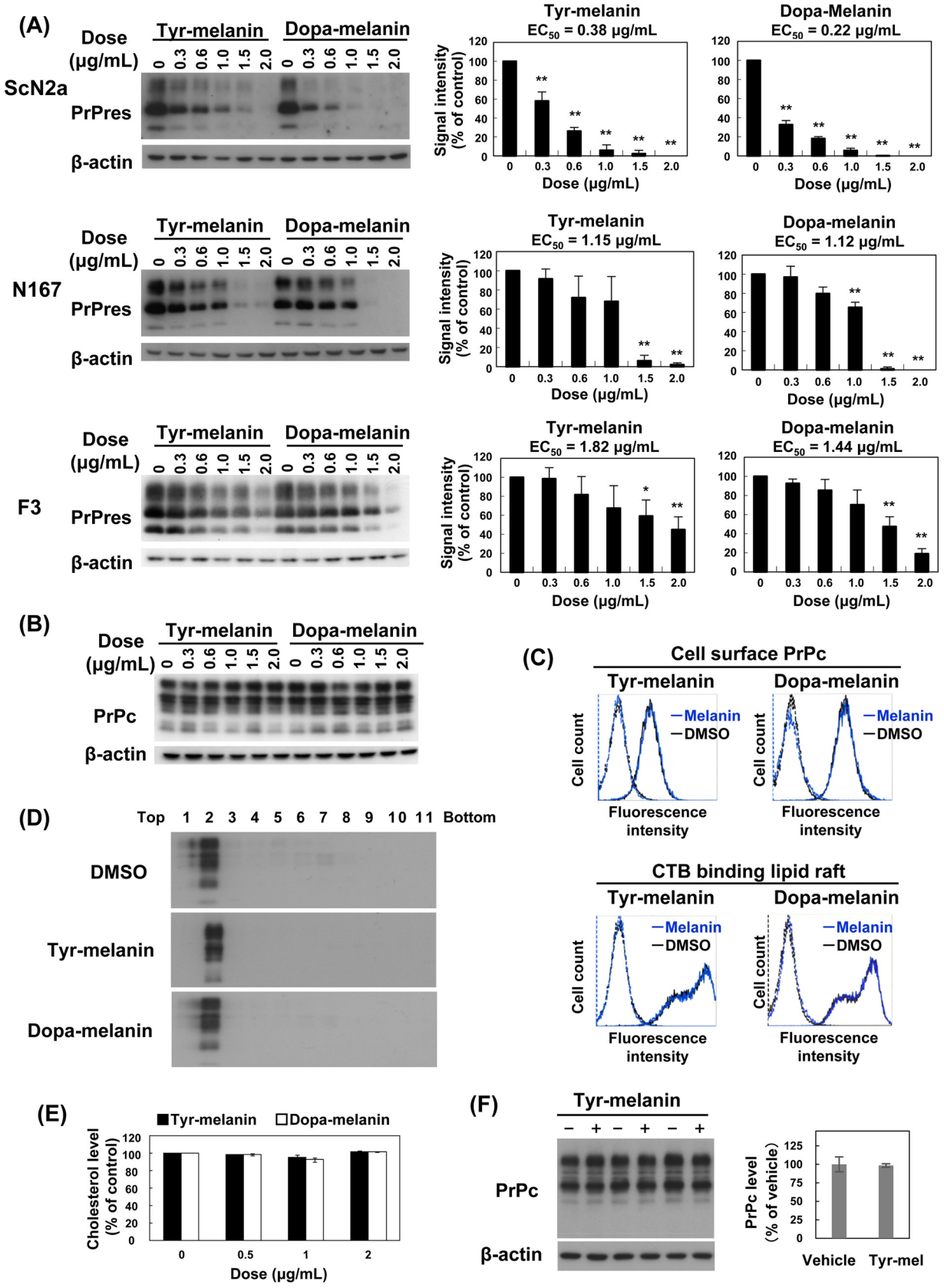

FIG 3 Antiprion activities of synthetic melanin compounds. (A) Immunoblot data for PrPres in three prion-infected cell lines treated with tyr-melanin or dopa-melanin. DMSO was used for the vehicle, and the amount of DMSO was adjusted in every cell culture well to a concentration of 0.2%. The bar graph shows averages and standard deviations for triplicate experiments (*, $P < 0.05$; **, $P < 0.01$). (B) Immunoblot data for PrPc

(Continued on next page)

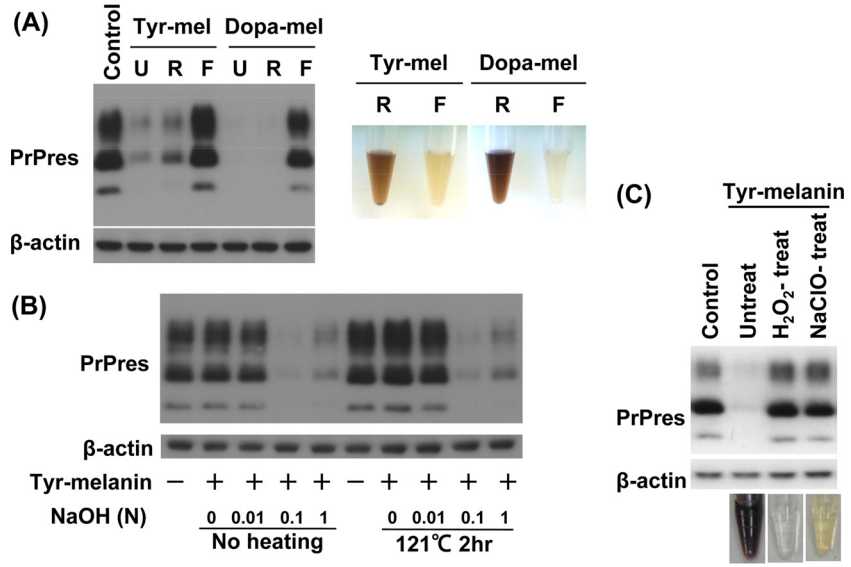

FIG 4 Characterization of the antiprion activities of melanin compounds. (A) Immunoblot data for PrPres in ScN2a cells treated with nonultrafiltrated (U) or ultrafiltrated melanin samples (retentate [R]) or filtrate [F]) from 1.5 μg/ml tyr-melanin or dopa-melanin. Ultrafiltration was performed with a 100-kDa cutoff membrane. The photo on the right shows the retentates and filtrates of melanin compound solutions. (B) Immunoblot data for PrPres in ScN2a cells treated with tyr-melanin, which had been treated with the designated concentrations of NaOH with or without autoclaving. Tyr-melanin was used at a concentration of 1.5 μg/ml in culture medium. Tyr-melanin was hardly solubilized in water or 0.01 N NaOH irrespective of heating. (C) Immunoblot data for PrPres in ScN2a cells treated with 1.5 μg/ml tyr-melanin that had been decomposed and decolored by treatment with H_2O_2 or NaClO.

predominantly localized in a fraction larger than 100 kDa (Fig. 4A). Because we were concerned that the method for obtaining extracts from insects might damage the chemical structure of melanin, synthetic melanin was similarly treated with sodium hydroxide alone or in combination with autoclaving. Melanin was hardly dissolved in water or 0.01 N sodium hydroxide, although it was thoroughly dissolved in 0.1 or 1 N sodium hydroxide, remaining soluble even after neutralization. This melanin solution displayed antiprion activity similar to that of dimethyl sulfoxide (DMSO)-dissolved melanin solution, and the antiprion activity was not affected by autoclaving (Fig. 4B). As in the sample of *C. chiron*, synthetic melanin lost its antiprion activity when it was bleached by treatment with NaClO or hydrogen peroxide (Fig. 4C). These data suggest that the antiprion active substances of our insect extract samples are comparable with those of synthetic melanin compounds.

Autophagy is reported to regulate abnormal PrP clearance (37). Thus, we examined whether autophagosome formation is enhanced in melanin-treated ScN2a cells. Consequently, melanin did not enhance autophagosome-related LC3-II levels in the cells (Fig. 5A). In contrast, while lysosome is also reported to regulate abnormal PrP clearance (38), lysosomal maturation, acidification, and overall degradation capacity are reportedly inhibited because of the inability of Rab7 to attach to vesicular membranes in prion-infected cells (39). Thus, we examined whether these impairments are reversed

FIG 3 Legend (Continued)
in N2a cells treated with tyr-melanin or dopa-melanin. (C) Flow cytometry of cell surface PrPc or cholera toxin B (CTB) binding lipid rafts in N2a cells treated with melanin compounds or vehicle (DMSO). Tyr-melanin or dopa-melanin was used at a concentration of 1.5 μg/ml. Blue and black lines indicate melanin- and DMSO-treated cells, respectively. The broken-line peaks on the left show their respective isotype controls. (D) Immunoblot data for PrPc fractionated by the flotation assay in N2a cells treated with melanin compounds or vehicle (DMSO). Tyr-melanin or dopa-melanin was used at a concentration of 1.5 μg/ml. Fraction numbers are indicated from the top to the bottom. (E) Cholesterol levels in N2a cells treated with melanin compounds or vehicle. The data show averages and standard deviations for triplicate experiments. No statistically significant difference was observed in any group comparisons. (F) Immunoblot data for pulse-chased, internalized cell surface PrPc in N2a cells treated with 1.5 μg/ml tyr-melanin or vehicle (DMSO). Biotin-labeled cell surface PrPc was chased for 15 min, and internalized PrPc was captured and analyzed. Triplicate experiment data are shown. The bar graph shows averages and standard deviations of the data, and no statistically significant difference was observed between groups.

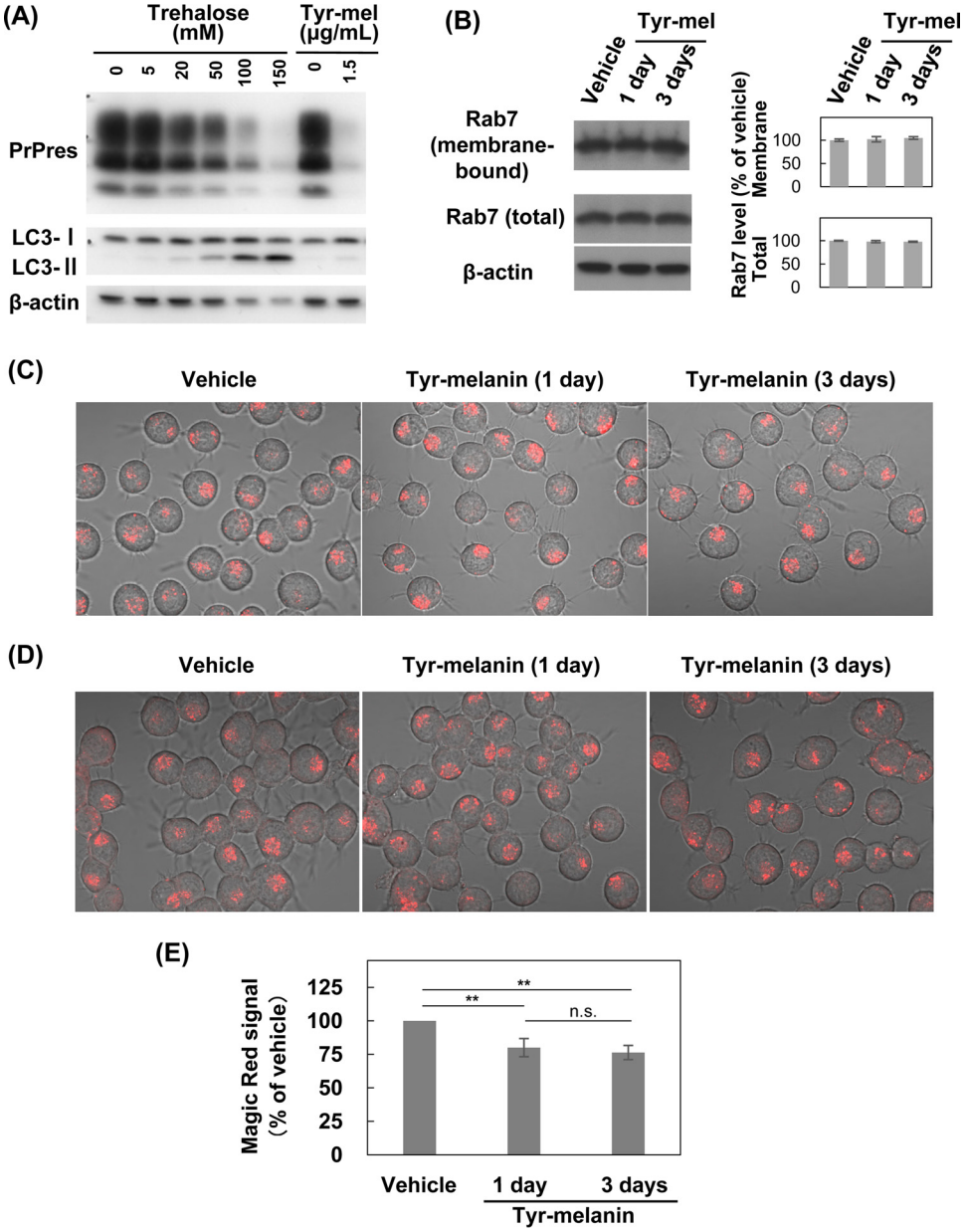

FIG 5 Autophagy or lysosomal function in melanin-treated cells. (A) Immunoblot data for autophagosome-related LC3-II in ScN2a cells treated with tyr-melanin. Trehalose-treated cell samples are shown as positive controls. (B) Immunoblot data for membrane-bound and total Rab7 in ScN2a cells treated with 1.5 μg/ml tyr-melanin for designated periods. The bar graph shows averages and standard deviations for triplicate experiments. No statistically significant difference was observed among groups. (C) Fluorescence microscopic images of lysosomes in ScN2a cells treated with 1.5 μg/ml tyr-melanin for designated periods. Lysosomes were stained with Lysotracker Red DND-99, which accumulates in a pH-dependent manner in lysosomes. (D) Fluorescence microscopic images of cathepsin B activity in ScN2a cells treated with 1.5 μg/ml tyr-melanin for designated periods. Cleavage activity was observed for Magic Red cathepsin B substrate MR-RR2. (E) Cathepsin B activity in ScN2a cells treated with 1.5 μg/ml tyr-melanin for designated periods. Cleavage activity for Magic Red cathepsin B substrate MR-RR2 was quantitatively analyzed by fluorescence plate reader in triplicate experiments (n.s., not significant; **, $P < 0.01$).

and whether lysosomal function is enhanced in melanin-treated ScN2a cells. We found that melanin did not modify the membrane-bound Rab7 expression levels (Fig. 5B), did not modify the number of vesicles accumulating Lysotracker dye (Fig. 5C), and did not enhance but rather reduced cathepsin B activity (Fig. 5D and E). These data suggest that melanin maintains antiprion activity without enhancing autophagy or lysosomal function.

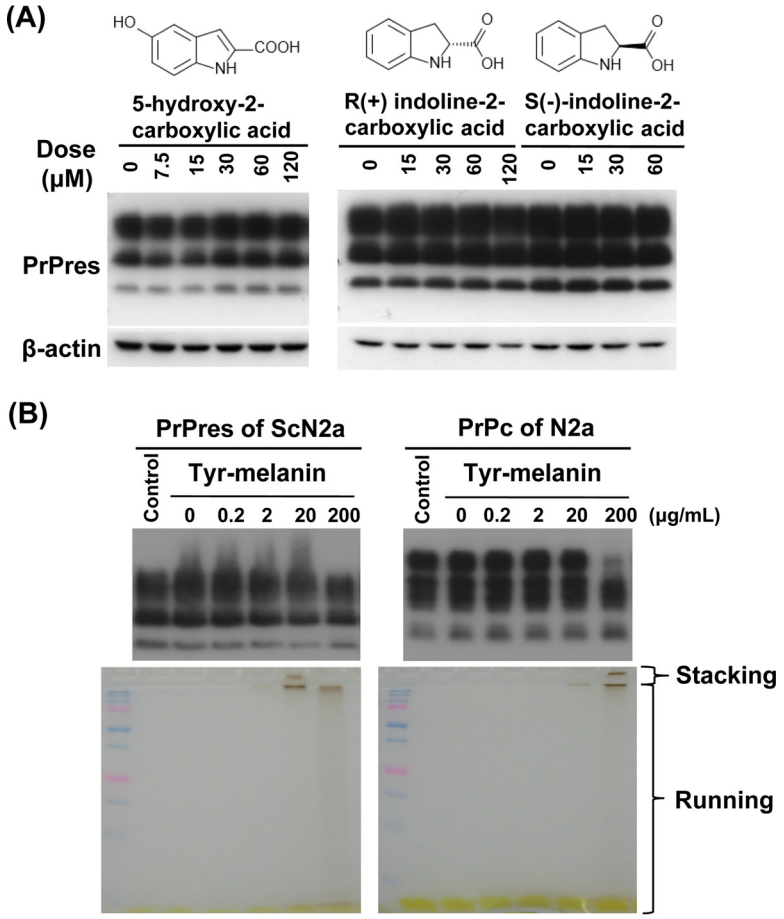

FIG 6 Association of other factors with the antiprion activity of melanin. (A) Immunoblot data for PrPres in ScN2a cells treated with the representative indole compounds. (B) Immunoblot data for PrPres or PrPc from cell lysates directly incubated with tyr-melanin. The amount of DMSO was adjusted in every cell lysate excluding "control" to a concentration of 2%. Respective SDS-PAGE gels used for blotting are shown below the immunoblots.

In contrast, indole structures such as decarboxylated indole and 2-carboxyl indole are commonly observed moieties in eumelanin (Fig. 2F). In addition, some indole derivatives are known to inhibit abnormal PrP formation in prion-infected cells (40). Thus, we examined whether the indole moieties themselves might play a role in the antiprion activity of insect extract samples and synthetic melanin compounds. However, no antiprion activity was observed for three representative indole compounds: 5-hydroxy-2-carboxylic acid, (*R*)-indoline-2-carboxylic acid, and (*S*)-indoline-2-carboxylic acid (Fig. 6A). Meanwhile, compounds such as tetracyclines (41) and polycationic compounds (42) reportedly convert abnormal PrP molecules into less-protease-resistant PrP molecules when cell lysates containing abnormal PrP molecules are incubated with these compounds. Therefore, we tested whether melanin modifies the protease sensitivity of abnormal PrP molecules. The results revealed that melanin did not change the protease sensitivity of melanin-incubated abnormal PrP molecules. Instead, some PrPc molecules exhibited disturbed mobility in SDS-PAGE gel following incubation with a high concentration of melanin (Fig. 6B).

Interaction between melanin and PrP. According to the results illustrated in Fig. 6B, it was presumable that melanin has affinity for PrP, especially PrPc. We tested this presumption using melanin-bound resin (melanin-SP) and other control resins. Consequently, PrPc but not abnormal PrP had affinity for melanin-SP, although both PrPc and abnormal PrP had affinity for DEAE-bound resin (Fig. 7A). This affinity was reduced in accordance with increasing proton concentrations, indicating electrostatic interactions

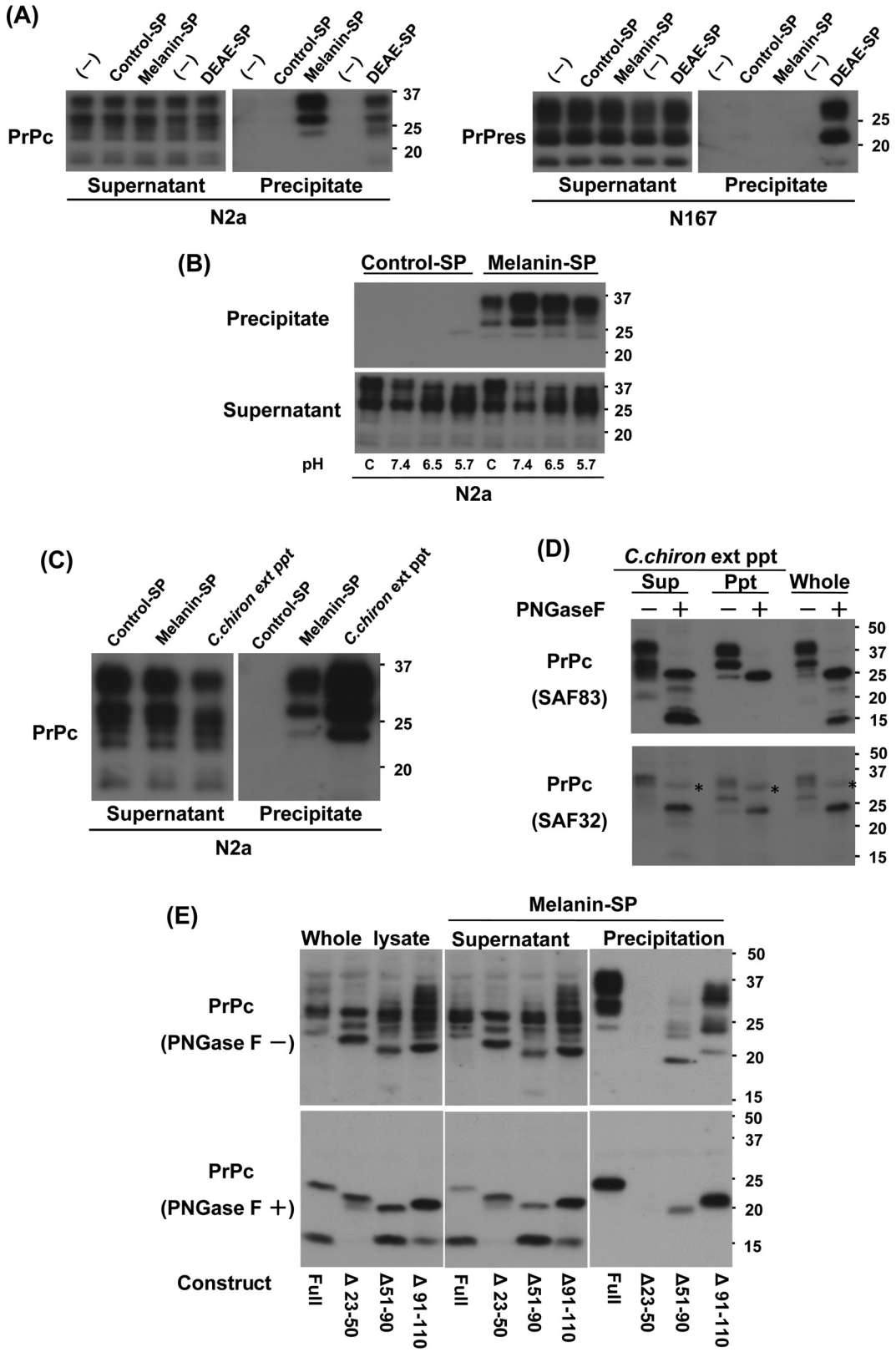

FIG 7 Interaction between melanin and PrP. (A) Immunoblot data for PrP absorbed from N2a or N167 cell lysates by melanin-Sepharose or other Sepharose beads. For PrPres detection, N167 cell lysates were first absorbed by Sepharose beads, and then both the supernatant and precipitate were digested with proteinase K. Control Sepharose and DEAE-Sepharose were used as negative and positive controls, respectively. (B) Immunoblot data for PrPc absorbed from N2a cell lysate by melanin-Sepharose under different pH conditions. Instead of normal lysis buffer as shown in panel C (0.5% deoxycholate, 0.5% NP-40 in PBS, pH 7.4), lysis buffer containing 1% NP-40 in 10 mM phosphate buffer was used for testing the effects of pH (pH

(Continued on next page)

between melanin and PrPc (Fig. 7B). Fine precipitates of the sample of *C. chiron*, which appeared during relatively long-term storage at 4°C, produced results similar to those obtained with melanin-SP (Fig. 7C). These results are consistent with previous results suggesting that the active components of the insect extracts are melanin or melanin-like substances.

Either melanin-SP or *C. chiron* extract-derived precipitates had affinity for PrPc molecules of 24 kDa or larger (Fig. 7A and C). Because multiple bands of PrPc represent both heterogeneously glycosylated PrPc and heterogeneously truncated PrPc, we compared PrPc signals after enzymatic deglycosylation. The anti-PrP antibodies SAF83 and SAF32, which recognize epitopes within mouse PrP residues 125 to 163 and 58 to 88, respectively, detected a single PrPc band of 24 kDa but not truncated PrPc bands smaller than 24 kDa after enzymatic deglycosylation (Fig. 7D). The results suggest that either a *C. chiron* extract melanin-like substance or synthetic melanin binds to full-length PrPc but not to the C-terminal fragments of PrPc.

Using deletion mutants of PrPc expressed in PrP-less HpL3-4 neuronal cells, we identified the PrPc domains that interact with melanin (Fig. 7E). Mutant PrPc with deletion of residues 23 to 50 (Δ23–50) lost affinity for melanin. Mutant PrP with deletion of residues 51 to 90 (Δ51–90) had relatively weak affinity for melanin compared to full-length PrPc or mutant PrP with deletion of residues 91 to 110 (Δ91–110). As demonstrated previously, after deglycosylation, SAF83 detected a single untruncated band of mutant PrPc or full-length PrPc of 19 to 24 kDa in size, although SAF83 did not detect a truncated PrPc band of approximately 16 kDa in size, which corresponds to the C1 peptide fragment. These data indicate that melanin has strong affinity for the N-terminal region containing a positively charged cluster, as well as weak affinity for the octarepeat peptide region.

Efficacy of melanin *in vitro* and *in vivo*. From the previously presented data, it was presumable that melanin inhibits abnormal PrP formation through a direct interaction with the N-terminal portion of PrP in prion-infected cells. Then, we further examined whether melanin modifies the conversion of PrPc to abnormal PrP *in vitro*. The results illustrated that melanin did not modify the conversion reaction during protein misfolding cyclic amplification (PMCA) within a concentration range (2 to 20 μg/ml) in which the vehicle did not affect the reaction (Fig. 8A).

Next, as the incidence of prion disease is reportedly much higher in white people than in black people (11), we were interested in investigating whether melanin in the periphery modifies the progression of the disease in prion-infected animals. We tested two animal models: an endogenous melanin-lacking model and a model injected exogenously with melanin. Albino B10.C-Tyr<c>/Hir mice, lacking melanin production in melanocytes and retinal pigment epithelial cells, and control C57BL/10JMsHir mice were used to compare survival times after intracerebral or intraperitoneal infection with the prion strain 22L. As shown in Fig. 8B, no significant difference was observed between these two mouse groups following intracerebral infection (163.8 $\pm$ 3.1 days in albino female mice versus 164.0 $\pm$ 4.5 days in control female mice, $P = 0.84$ in log-rank test; 167.4 $\pm$ 1.9 days in albino male mice versus 164.6 $\pm$ 5.4 days in control male mice, $P = 0.39$) or intraperitoneal infection (248.3 $\pm$ 6.4 days in albino female mice versus 249.5 $\pm$ 26.5 days in control female mice, $P = 0.75$; 261.6 $\pm$ 8.5 days in albino male mice versus 264.1 $\pm$ 24.4 days in control male mice, $P = 0.12$). Meanwhile, a tolerance dose injection of tyr-melanin (50 mg) was performed 3 days after intraperitoneal infection with prion strain 263K in hamster PrP-overexpressing Tg7 mice. As shown in Fig. 8C,

FIG 7 Legend (Continued)
5.7, 6.5, and 7.4). (C) Immunoblot data for PrPc absorbed from N2a cell lysate by *C. chiron* extract-derived precipitation. (D) Immunoblot data for the deglycosylation products of PrPc absorbed from N2a cell lysate by *C. chiron* extract-derived precipitation. SAF83 recognizing an epitope within mouse PrP residues 125 to 163 was first used for probing PrP signals. Then, subsequent to stripping the antibody, SAF32 recognizing an epitope within mouse PrP residues 58 to 88 was used for reprobing. Nonspecific signals are indicated by asterisks. (E) Immunoblot data for PrPc absorbed from the PrP deletion mutant-expressing HpL3-4 cell lysates by melanin-Sepharose. Data for PrPc before or after enzymatic deglycosylation (PNGase F $-$ or $+$) are shown. PrPΔ23–50 did not contain a C1 fragment as previously reported (87).

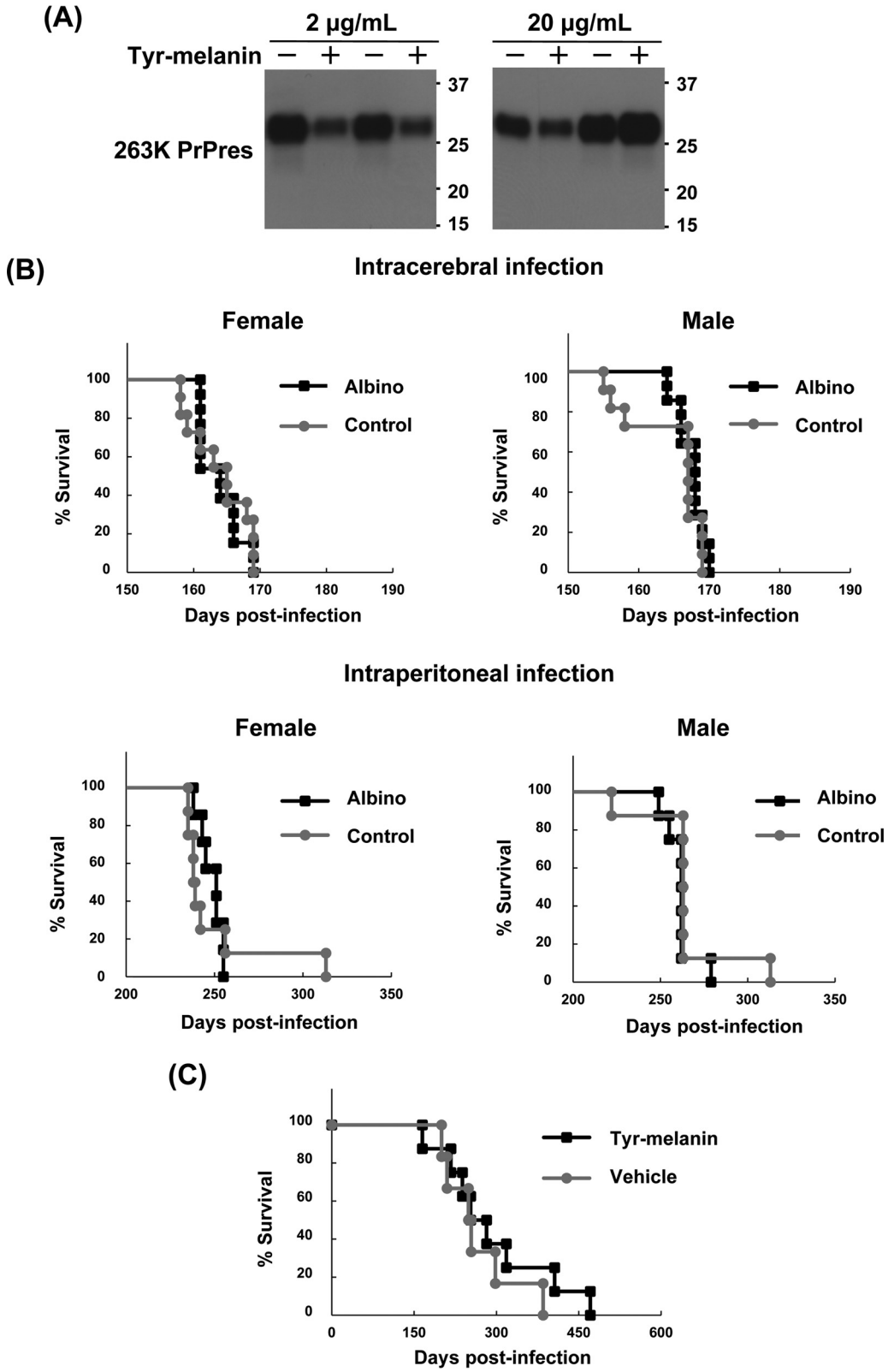

FIG 8 Efficacy of melanin *in vitro* and *in vivo*. (A) Immunoblot data for 263K prion-derived PrPres after PMCA reaction in the presence of tyr-melanin. Representative data from duplicate experiments are shown. Anti-PrP monoclonal antibody 3F4 was used for PrP detection. (B) Kaplan-Meier graph of the albino and control animals. Both albino B10.C-Tyr<c>/Hir and control C57BL/10JMsHir mice were infected intracerebrally or intraperitoneally with 22L prion and observed until the disease became terminal. (C) Kaplan-Meier graph of animals treated with melanin. Female Tg7 mice intraperitoneally infected with 263K prion were given a single subcutaneous injection of tyr-melanin at a tolerance dose (50 mg) or vehicle 3 days postinfection and observed until the disease became terminal.

melanin treatment did not affect the survival times of the mice (293.8 ± 101.4 days in the melanin-treated group versus 266.0 ± 68.0 days in the vehicle group, $P = 0.44$). Pharmacokinetics of injected melanin was not evaluated, but the bioavailability of injected melanin was likely limited because a large portion of injected melanin remained around the subcutaneous injection site on the backs of animals until the disease progressed to the end stage.

DISCUSSION

In the present study, we found that black- to dark brown-colored water-soluble extracts from insect materials inhibited abnormal PrP formation in prion-infected cells. Representative extract samples displayed concentration-dependent antiprion activities. The antiprion components in these samples were implicated to be melanin or a melanin-like substance based on the data; specifically, the antiprion components were high-molecular-weight molecules that were resistant to a strong hydrolytic condition and digestive treatments with chitinase, zymolyase, and proteinase K, sensitive to bleaching treatment, and negatively charged. Thereafter, synthetic melanin compounds produced data consistent with those of the insect samples. Consequently, we concluded that melanin, especially eumelanin, exerts antiprion activity in prion-infected cells.

Melanin, a pigment distributed in most organisms, has a heterogeneous chemical structure produced by the oxidation of tyrosine and tyrosine derivatives followed by polymerization (43). Eumelanin is the most common type of melanin, and it is contained in black or brown biological substances. It comprises numerous cross-linked 2-carboxyl indole and decarboxylated indole polymers (Fig. 2F), although another type of melanin, pheomelanin, is a cysteine-containing red-brown polymer of benzothiazine units. In the case of insects, eumelanin is synthesized for the formation of body color, insect innate immunity against invading pathogens, and insect hemostasis (44). In insect cuticles, eumelanin is involved in brown-black pigmentation and cuticle hardening during the ecdysis process. Therefore, it is presumable that melanin, especially eumelanin, is a predominant component in the extracts of tested insect materials, including cicada shells.

Regarding the mechanism by which melanin alters abnormal PrP formation in prion-infected cells, melanin did not affect abnormal PrP formation-related factors such as total and cell surface PrPc levels, cell surface PrPc turnover, cholesterol and lipid raft microdomain levels, and autophagosome levels. Melanin also did not enhance lysosomal function. The present study has revealed that melanin has strong affinity for the PrP N-terminal region, including a positively charged cluster (amino acids 23 to 28), as well as weak affinity for the octarepeat peptide region (amino acids 51 to 91). This interaction is similar to that of heparin, a representative polyanionic glycan known to inhibit abnormal PrP formation in prion-infected cells. In our previous report (45), a disaccharide unit of heparin, (2-deoxy-2-sulfoamido-6-*O*-sulfo-α-D-glycopyranosyl)-(1–4)-*O*-(2-*O*-sulfo-α-L-idopyranosyluronic acid), influenced the potency for inhibiting the formation of abnormal PrP and exerted strong affinity for the N-terminal portion of PrP (PrP residues 23 to 89). Therefore, it is strongly suggested that melanin and heparin inhibit the conversion of PrP by directly interacting with the N terminus of PrP as previously implicated for other anionic antiprion compounds (46–49).

Coincident findings for melanin and heparin were also observed in the results of PMCA using the hamster-adapted scrapie prion 263K. In the present study, melanin did not modify the conversion reaction in PMCA within a concentration range in which the vehicle did not affect the PMCA reaction. In PMCA reactions, polyanionic substances such as RNA and sulfated glycans reportedly modify the conversion of PrPc to abnormal PrP (50–52). However, heparin reportedly enhances the PMCA reaction for the variant Creutzfeldt-Jakob disease prion, but it does not modify the reaction for the hamster-adapted scrapie prion 263K (50). These findings suggest that agents that interact with the PrP N-terminal domain might not modify the *in vitro* PrP conversion reaction for

prion 263K, and this effect might be prion strain dependent. However, this implication remains to be further evaluated.

In humans and other animals, melanin and melanin-related metabolites are produced in a specialized group of cells, such as melanocytes and retinal pigment epithelial cells. It is known that most of these melanin compounds are retained in the cells, but some are secreted into blood, circulated in the body, and then excreted into urine in accordance with the degree of pigmentation in the body (53–55). Meanwhile, an epidemiological study on human prion diseases in the United States revealed that the age-adjusted incidence of human prion diseases for white people is 2.7-fold higher than that for black people (11). These findings imply that melanin might be an endogenous factor influencing racial variations in the incidence of human prion diseases. However, to our knowledge, neither endogenous melanin in a physiological condition nor exogenous melanin in a tolerance dose altered the disease course of prion diseases, even when prions were inoculated via a peripheral route. Thus, it is suggested that melanin, a main determinant of skin color, does not modify prion disease pathogenesis.

Conversely, melanin in the brain is observed in a limited number of cells: meningeal melanocytes in localized areas of the meninges (56) and catecholaminergic neurons of the substantia nigra and locus coeruleus in the brainstem (57). Meningeal melanocytes are reportedly distributed sparsely in the meninges surrounding the olfactory bulb, the meninges between the cerebellum and cortex, and the cranial floor meninges surrounding the pterygopalatine artery in mice (56). Catecholaminergic neurons contain melanin called neuromelanin, which is biosynthesized in complicated pathways that vary from those of peripheral melanin (58, 59). Thus, albinos who lack tyrosinase display normally pigmented substantia nigra (60) but have no pigmented cells in the meninges (56). Neuromelanin concentrations increase during aging (61), and human brains contain the largest amounts of neuromelanin; however, lesser amounts are reported in other primates (57). Neuromelanin appears to be absent or present only in very small amounts in mice and many other species (57, 62). We examined the substantia nigra by Fontana-Masson staining and observed no positive signal in the brain of either albino or control black mice in the current study (data not shown), although histochemically stained signals for neuromelanin have been reported in the substantia nigra of aged mouse brains (63). Because the brainstem regions in humans, including substantia nigra and locus coeruleus, are primarily spared from neurodegenerative changes owing to a prion disease (64), it is interesting to consider whether neuromelanin is protective against prion formation in the brain.

The positively charged cluster (amino acids 23 to 28) and octapeptide repeat region (amino acids 51 to 91) at the N-terminal portion of PrPc are reportedly capable of interacting with many endogenous factors such as metal ions (65–69), anionic lipids (70–72), nucleic acids (73–76), sulfated glycosaminoglycans (77–79), hemin (80), and proteins, including low-density lipoprotein receptor-related protein 1 (81), abnormal PrP (82, 83), and Aβ oligomers (84). These interactions are suggested to be associated with multiple functions such as PrPc endocytosis, PrPc nuclear targeting, neuroprotection, neurotoxicity, transduction of polypeptides, antimicrobial activity, DNA transfer, and PrP conversion (85). In addition, the positively charged cluster is reported to regulate the efficiency of α-cleavage (86–88), which leads to the release of the PrP N1 peptide (amino acids 23 to 110), which possesses neuroprotective activity (83, 89, 90). Thus, melanin might be capable of interfering with these interactions and be a useful tool for elucidating their functions.

In conclusion, the findings newly identify melanin as a factor that interacts with the N terminus of PrP. The pathophysiological roles of the melanin-PrP interaction remain unclear, but peripheral melanin is incapable of modifying the disease course of prion disease in mice. The findings suggest that peripheral melanin or skin color is not a relevant factor regarding why the incidence of human prion disease is much higher in white people than in black people.

MATERIALS AND METHODS

Insect extracts and synthetic compounds. Insects or insect parts were obtained from a local insect shop or around the laboratory. They included adults of the following species: *Agrus convolvuli* (large hawk-moth), *Allomyrina dichotoma* (Japanese horned beetle), *Chalcosoma chiron* (Caucasus beetle), *Graptopsaltria nigrofuscata* (large brown cicada), *Halyomorpha halys* (brown marmorated stink bug), and *Papilio protenor* (spangle butterfly). They also included larvae of *Dorcus hopei binodulosus* (Japanese stag beetle) and the larval shell of *Graptopsaltria nigrofuscata*. They were frozen for euthanasia and chopped into pieces. Insect materials were immersed in 10 volumes of 1 N NaOH and autoclaved at 121°C for 4 h. After neutralization, the extract solution was dialyzed with distilled water. After centrifugation at 20,000 × *g*, a black- or dark brown-colored extract solution was obtained and stored at 4°C until use.

Hydroxypropyl chitin was synthesized from chitin (Wako Pure Chemical Industries, Osaka, Japan) as described previously (91). Synthetic melanin derived from tyrosine (tyr-melanin) was purchased (Sigma-Aldrich, St. Louis, MO), and synthetic melanin produced from 3-hydroxy-L-tyrosine (dopa-melanin) was synthesized as described previously (92).

Analyses of PrP and other factors in cells. We used N2a mouse neuroblastoma cells as well as three types of distinct prion strain-infected N2a-derived cells: ScN2a cells infected with prion RML, N167 cells infected with prion 22L, and F3 cells infected with prion Fukuoka-1. N167 and F3 cells derived from N2a#58 cells express 5-fold the PrPc levels of N2a or ScN2a cells (22, 23). Cells were treated with the test materials for 3 days (i.e., from cell seeding to time of confluence) or other defined time periods if stated, as previously described (93–95). Cell lysate was prepared using lysis buffer (0.5% sodium deoxycholate, 0.5% Nonidet P-40, phosphate-buffered saline [PBS], pH 7.4). The toxicity of test compounds to cells was evaluated by assaying protein concentrations in the cell lysates, as described previously (96). The amounts of PrPres, PrPc, or β-actin in the cell lysates were analyzed using immunoblotting with anti-PrP monoclonal antibody SAF83 (Bertin Pharma, Montigny-le-Bretonneux, France) or anti-β-actin monoclonal antibody, as described previously (96). To analyze cell surface PrPc or lipid raft microdomain levels, flow cytometry was performed with N2a cells using anti-PrP monoclonal antibody SAF83 or fluorescence-conjugated cholera toxin B as described previously (96). A flotation assay of detergent-insoluble membrane complexes was also performed to analyze the distribution of lipid raft-associated PrPc as described previously (96, 97). The cholesterol content of cells was analyzed as described previously (98).

Cell surface PrPc internalization was analyzed as described previously (99). Briefly, cell surface molecules were biotinylated with 1 mg/ml EZ-Link Sulfo-NHS-SS-Biotin (Thermo Fisher Scientific Inc., Waltham, MA) in PBS (pH 8.0) at 4°C for 30 min and subsequently washed with 100 mM glycine in PBS to quench free sulfo-biotin. Cells were incubated at 37°C for 15 min in a culture medium containing 1.5 μg/ml tyr-melanin or vehicle to internalize cell surface molecules. Subsequently, to remove disulfide-linked biotin from the cell surface, cells were incubated twice at 4°C for 30 min in 20 mM sodium 2-mercaptoethanesulfonate solution (containing 150 mM NaCl, 20 mM Tris-HCl [pH 8.6], 1 mM EDTA, and 0.2% bovine serum albumin) and once at 4°C for 15 min in Hanks' balanced salt solution containing 20 mM iodoacetamide. Cell lysates were then prepared with lysis buffer, and biotinylated molecules were captured with avidin beads. Captured molecules were analyzed by immunoblotting with the anti-PrP antibody SAF83, as described previously (96).

As an indicator of autophagy, autophagosome formation was analyzed in cells by immunoblotting for microtubule-associated protein 1A/1B-light chain 3 (LC3), as previously described (96). Membrane-bound Rab7 expression, lysosomal acidification, and lysosomal enzyme activity were all analyzed in cells as factors associated with lysosomal function. Because membrane-bound Rab7 expression is reportedly reduced in prion-infected cells, resulting in impaired lysosomal maturation and degradation capacity (39), membrane-bound Rab7 expression and total Rab7 expression were analyzed together by immunoblotting with anti-Rab7 antibody (Cell Signaling Technology, Danvers, MA). Crude membrane fractions were prepared for analyzing membrane-bound Rab7, as described previously (39), and cell lysate for analyzing total Rab7 was prepared with the lysis buffer. Lysosomal acidification, also reportedly reduced in prion-infected cells (39), was analyzed by fluorescence microscopy. Cells were stained with Lysotracker Red DND-99 (Thermo Fisher Scientific Inc.), which accumulates in lysosomes in a pH-dependent manner. As a representative lysosomal enzyme, cathepsin B was examined. Activity was visualized in cells by Magic Red cathepsin B substrate MR-RR2 (Immunochemistry Technologies, Bloomington, MN) and then analyzed by fluorescence microscopy or fluorescence plate reader, according to the manufacturer's instruction.

Analysis of insect extracts. For chemical property evaluation via digestive treatments, insect extracts were treated with chitinase (120 μg/ml; Sigma-Aldrich), zymolyase (180 μg/ml; Nacalai Tesque, Kyoto, Japan), or proteinase K (90 μg/ml; Merck Millipore, Darmstadt, Germany) at 37°C for 30 h. Each enzymatic reaction was stopped by heat treatment at 95°C for 10 min. For the evaluation using bleach treatment, each insect extract was treated with 4% NaClO at room temperature for 2 weeks. The reaction solution was neutralized and dialyzed with distilled water.

Molecular weight fractionation of insect extracts or synthetic melanin compounds was performed using centrifugal ultrafiltration devices (Merck Millipore).

Mechanism of the antiprion action of melanin. Melanin was treated with 4% NaClO or 27% H_2O_2 solution at room temperature for 2 weeks. After neutralization and dialysis with deionized water, each sample was added to cells at a final concentration of 1.5 μg/ml.

Melanin-Sepharose was prepared using 18 mg of tyr-melanin in 0.1 N NaOH, which was coupled with 250 mg of epoxy-activated Sepharose 6B (GE Healthcare, Little Chalfont, UK) according to the manufacturer's instructions. Control Sepharose was prepared using no substrate in 0.1 N NaOH coupled with epoxy-activated Sepharose 6B. DEAE-Sepharose was purchased from GE Healthcare. The batch or spin

cup method was used for affinity purification. Briefly, 100 μl of N2a cell lysate was applied to a Sepharose gel slurry corresponding to 600 μg of dry beads and incubated for 1 h in a tube or spin cup column. Double volumes of cell lysate and gel slurry were used for abnormal PrP detection from N167 cells. After centrifugation, supernatant was used for immunoblot analysis, and precipitated gel was prepared for immunoblot analysis after washing twice with lysis buffer. For PrPres detection, either 120 μl of supernatants or precipitates resuspended in 120 μl of lysis buffer were treated with proteinase K as previously described (96). Immunoblotting was performed by using antiPrP monoclonal antibody SAF83, recognizing an epitope within mouse PrP residues 125 to 163, or SAF32, recognizing an epitope within mouse PrP residues 58 to 88 (Bertin Pharma), as previously described (96). Regarding the deglycosylation of PrP molecules, samples were digested for 2 h with the recombinant glycopeptide *N*-glycosidase F (PNGase F; New England BioLabs, Ipswich, MA) according to the manufacturer's instructions.

Expression of PrP deletion mutant. Full-length mouse PrP (residues 23 to 231) DNA was cloned from mouse genomic DNA using PCR and inserted into a pcDNA mammalian expression vector (Invitrogen, Carlsbad, CA). Subsequently, this expression vector was used to obtain three types of PrP deletion mutant expression vectors by PCR: N terminus-deleted mutant PrP (PrPΔ23–50), octarepeat region-deleted mutant PrP (PrPΔ51–90), and middle region-deleted mutant PrP (PrPΔ91–110). The sequence was confirmed using a DNA sequencer. These expression vectors were introduced into PrP-less HpL3-4 neuronal cells (100) using TransFectin Lipid Reagent (Bio-Rad, Hercules, CA), and transiently expressed PrP molecules were assayed by immunoblotting with anti-PrP monoclonal antibody SAF83.

Protein misfolding cyclic amplification. According to a previously described method (50), a reaction mixture containing 0.1% 263K prion-infected hamster brain homogenate and 10% normal hamster brain homogenate was subjected to 96 cycles of sonication and incubation with an automatic cross-ultrasonic apparatus (Elestein 070-GOTW; Elekon Science Corp., Chiba, Japan). Tyr-melanin in DMSO was added to the reaction mixture before starting the PMCA reactions at a concentration of 2 or 20 μg/ml. After the reactions, the samples were digested with 100 μg/ml proteinase K at 37°C for 1 h, and the levels of PrPres were detected by immunoblotting using anti-hamster PrP monoclonal antibody 3F4 (BioLegend, Inc., San Diego, CA).

Animal study. Both albino B10.C-Tyr<c>/Hir (101) and control C57BL/10JMsHir mice were provided by the Riken BRC through the National Bio-Resource Project of the MEXT, Japan. Eight- to ten-week-old B10.C-Tyr<c>/Hir and C57BL/10JMsHir mice were intracerebrally or intraperitoneally infected with 20 or 100 μl, respectively, of 1% brain homogenate from a prion 22L-infected terminally ill mouse. The animals were monitored daily until the disease became terminal, at which time the mice were akinetic (with a lack of grooming behavior, coordination, and parachute reaction) or exhibited a rigid tail, an arched back, and weight loss of approximately 10% within 1 week. The survival time, which was defined in this study as the duration from infection to terminal disease, was assayed. Similarly, 8- to 10-week-old female Tg7 mice overexpressing hamster PrPc (102), which were kindly provided by Bruce Chesebro of the Laboratory of Persistent Viral Diseases of NIAID's Rocky Mountain Laboratories (Hamilton, MT), were used to analyze the effectiveness of exogenously administered melanin. A single bolus of a 100-μl solution containing a mixture of tyr-melanin (50 mg) and albumin (10 mg) was injected subcutaneously into the backs of mice 3 days postintraperitoneal infection. Infection was achieved via inoculation with 100 μl of the 1% brain homogenate of a prion 263K-infected terminally ill hamster.

The animal experiments described in this study were performed in accordance with the Guidelines for Animal Experimentation of Tohoku University under the review and approval of the Institutional Animal Care and Use Committee of Tohoku University (approval numbers 2013MdA-194 and 2015MdA-191).

Statistical analysis. Data were evaluated on the basis of the results of triplicate experiments using one-way analysis of variance followed by Dunnett's test or the Tukey-Kramer method for multiple-group comparisons or using *t* test for two-group comparisons. The survival rate was calculated using the Kaplan-Meier method, and significance was evaluated using the log rank method as previously described (103).

ACKNOWLEDGMENTS

We thank Yuka Fujiwara, Yukino Funayama, and Chiemi Yoshida for technical assistance.

This work was supported by the Ministry of Health, Labor and Welfare of Japan (nanchi-ippan-H22-009/-H26-017), the Japan Society for the Promotion of Science (22390172), and a Cooperative Research Grant of the Institute for Enzyme Research, Tokushima University.

We declare that we have no conflicts of interest.

REFERENCES

1. Prusiner SB. 1998. Prions. Proc Natl Acad Sci U S A 95:13363–13383. https://doi.org/10.1073/pnas.95.23.13363.
2. Teruya K, Doh-ura K. 2013. Amyloid-binding compounds and their anti-prion potency. Curr Top Med Chem 13:2522–2532. https://doi.org/10.2174/15680266113136660178.
3. Sim VL. 2012. Prion disease: chemotherapeutic strategies. Infect Disord Drug Targets 12:144–160. https://doi.org/10.2174/187152612800100161.
4. Trevitt CR, Collinge J. 2006. A systematic review of prion therapeutics in experimental models. Brain 129:2241–2265. https://doi.org/10.1093/brain/awl150.
5. Geschwind MD, Kuo AL, Wong KS, Haman A, Devereux G, Raudabaugh

BJ, Johnson DY, Torres-Chae CC, Finley R, Garcia P, Thai JN, Cheng HQ, Neuhaus JM, Forner SA, Duncan JL, Possin KL, Dearmond SJ, Prusiner SB, Miller BL. 2013. Quinacrine treatment trial for sporadic Creutzfeldt-Jakob disease. J Neurol 81:2015–2023. https://doi.org/10.1212/WNL.0b013e3182a9f3b4.
6. Tsuboi Y, Doh-ura K, Yamada T. 2009. Continuous intraventricular infusion of pentosan polysulfate: clinical trial against prion diseases. Neuropathology 29:632–636. https://doi.org/10.1111/j.1440-1789.2009.01058.x.
7. Collinge J, Gorham M, Hudson F, Kennedy A, Keogh G, Pal S, Rossor M, Rudge P, Siddique D, Spyer M, Thomas D, Walker S, Webb T, Wroe S, Darbyshire J. 2009. Safety and efficacy of quinacrine in human prion disease (PRION-1 study): a patient-preference trial. Lancet Neurol 8:334–344. https://doi.org/10.1016/S1474-4422(09)70049-3.
8. Otto M, Cepek L, Ratzka P, Doehlinger S, Boekhoff I, Wiltfang J, Irle E, Pergande G, Ellers-Lenz B, Windl O, Kretzschmar HA, Poser S, Prange H. 2004. Efficacy of flupirtine on cognitive function in patients with CJD: a double-blind study. J Neurol 62:714–718. https://doi.org/10.1212/01.WNL.0000113764.35026.EF.
9. Haïk S, Marcon G, Mallet A, Tettamanti M, Welaratne A, Giaccone G, Azimi S, Pietrini V, Fabreguettes J-R, Imperiale D, Cesaro P, Buffa C, Aucan C, Lucca U, Peckeu L, Suardi S, Tranchant C, Zerr I, Houillier C, Redaelli V, Vespignani H, Campanella A, Sellal F, Krasnianski A, Seilhean D, Heinemann U, Sedel F, Canovi M, Gobbi M, Di Fede G, Laplanche J-L, Pocchiari M, Salmona M, Forloni G, Brandel J-P, Tagliavini F. 2014. Doxycycline in Creutzfeldt-Jakob disease: a phase 2, randomised, double-blind, placebo-controlled trial. Lancet Neurol 13:150–158. https://doi.org/10.1016/S1474-4422(13)70307-7.
10. Teruya K, Doh-ura K. 11 November 2016. Insights from therapeutic studies for PrP prion disease. Cold Spring Harb Perspect Med 2016:a024430. https://doi.org/10.1101/cshperspect.a024430.
11. Holman RC, Belay ED, Christensen KY, Maddox RA, Minino AM, Folkema AM, Haberling DL, Hammett TA, Kochanek KD, Sejvar JJ, Schonberger LB. 2010. Human prion diseases in the United States. PLoS One 5:e8521. https://doi.org/10.1371/journal.pone.0008521.
12. Lloyd SE, Mead S, Collinge J. 2013. Genetics of prion diseases. Curr Opin Genet Dev 23:345–351. https://doi.org/10.1016/j.gde.2013.02.012.
13. d'Aignaux JN, Cousens SN, Smith PG. 2001. Predictability of the UK variant Creutzfeldt-Jakob disease epidemic. Science 294:1729–1731. https://doi.org/10.1126/science.1064748.
14. Korth C, May BC, Cohen FE, Prusiner SB. 2001. Acridine and phenothiazine derivatives as pharmacotherapeutics for prion disease. Proc Natl Acad Sci U S A 98:9836–9841. https://doi.org/10.1073/pnas.161274798.
15. Kocisko DA, Baron GS, Rubenstein R, Chen J, Kuizon S, Caughey B. 2003. New inhibitors of scrapie-associated prion protein formation in a library of 2,000 drugs and natural products. J Virol 77:10288–10294. https://doi.org/10.1128/JVI.77.19.10288-10294.2003.
16. Doh-ura K, Kuge T, Uomoto M, Nishizawa K, Kawasaki Y, Iha M. 2007. Prophylactic effect of dietary seaweed Fucoidan against enteral prion infection. Antimicrob Agents Chemother 51:2274–2277. https://doi.org/10.1128/AAC.00917-06.
17. Hamanaka T, Sakasegawa Y, Ohmoto A, Kimura T, Ando T, Doh-ura K. 2011. Anti-prion activity of protein-bound polysaccharide K in prion-infected cells and animals. Biochem Biophys Res Commun 405:285–290. https://doi.org/10.1016/j.bbrc.2011.01.030.
18. Ezzati-Tabrizi R, Farrokhi N, Talaei-Hassanloui R, Alavi SM, Hosseininaveh V. 2013. Insect inducible antimicrobial peptides and their applications. Curr Protein Pept Sci 14:698–710.
19. Ratcliffe NA, Mello CB, Garcia ES, Butt TM, Azambuja P. 2011. Insect natural products and processes: new treatments for human disease. Insect Biochem Mol Biol 41:747–769. https://doi.org/10.1016/j.ibmb.2011.05.007.
20. Slocinska M, Marciniak P, Rosinski G. 2008. Insects antiviral and anticancer peptides: new leads for the future? Protein Pept Lett 15:578–585. https://doi.org/10.2174/092986608784966912.
21. Natori S. 1994. Function of antimicrobial proteins in insects. Ciba Found Symp 186:123–132.
22. Nishida N, Harris DA, Vilette D, Laude H, Frobert Y, Grassi J, Casanova D, Milhavet O, Lehmann S. 2000. Successful transmission of three mouse-adapted scrapie strains to murine neuroblastoma cell lines overexpressing wild-type mouse prion protein. J Virol 74:320–325. https://doi.org/10.1128/JVI.74.1.320-325.2000.
23. Ishikawa K, Doh-ura K, Kudo Y, Nishida N, Murakami-Kubo I, Ando Y, Sawada T, Iwaki T. 2004. Amyloid imaging probes are useful for detection of prion plaques and treatment of transmissible spongiform encephalopathies. J Gen Virol 85:1785–1790. https://doi.org/10.1099/vir.0.19754-0.
24. Lewis V, Hooper NM. 2011. The role of lipid rafts in prion protein biology. Front Biosci (Landmark Ed) 16:151–168. https://doi.org/10.2741/3681.
25. Bate C, Tayebi M, Williams A. 2010. Glycosylphosphatidylinositol anchor analogues sequester cholesterol and reduce prion formation. J Biol Chem 285:22017–22026. https://doi.org/10.1074/jbc.M110.108548.
26. Gilch S, Bach C, Lutzny G, Vorberg I, Schatzl HM. 2009. Inhibition of cholesterol recycling impairs cellular PrP(Sc) propagation. Cell Mol Life Sci 66:3979–3991. https://doi.org/10.1007/s00018-009-0158-4.
27. Kumar R, McClain D, Young R, Carlson GA. 2008. Cholesterol transporter ATP-binding cassette A1 (ABCA1) is elevated in prion disease and affects PrPC and PrPSc concentrations in cultured cells. J Gen Virol 89:1525–1532. https://doi.org/10.1099/vir.0.83358-0.
28. Pani A, Norfo C, Abete C, Mulas C, Putzolu M, Laconi S, Orru CD, Cannas MD, Vascellari S, La Colla P, Dessi S. 2007. Antiprion activity of cholesterol esterification modulators: a comparative study using ex vivo sheep fibroblasts and lymphocytes and mouse neuroblastoma cell lines. Antimicrob Agents Chemother 51:4141–4147. https://doi.org/10.1128/AAC.00524-07.
29. Gilch S, Nunziante M, Ertmer A, Schatzl HM. 2007. Strategies for eliminating PrP(c) as substrate for prion conversion and for enhancing PrP(Sc) degradation. Vet Microbiol 123:377–386. https://doi.org/10.1016/j.vetmic.2007.04.006.
30. Klingenstein R, Lober S, Kujala P, Godsave S, Leliveld SR, Gmeiner P, Peters PJ, Korth C. 2006. Tricyclic antidepressants, quinacrine and a novel, synthetic chimera thereof clear prions by destabilizing detergent-resistant membrane compartments. J Neurochem 98:748–759. https://doi.org/10.1111/j.1471-4159.2006.03889.x.
31. Bate C, Salmona M, Diomede L, Williams A. 2004. Squalestatin cures prion-infected neurons and protects against prion neurotoxicity. J Biol Chem 279:14983–14990. https://doi.org/10.1074/jbc.M313061200.
32. Taraboulos A, Scott M, Semenov A, Avrahami D, Laszlo L, Prusiner SB. 1995. Cholesterol depletion and modification of COOH-terminal targeting sequence of the prion protein inhibit formation of the scrapie isoform. J Cell Biol 129:121–132. https://doi.org/10.1083/jcb.129.1.121.
33. Marella M, Lehmann S, Grassi J, Chabry J. 2002. Filipin prevents pathological prion protein accumulation by reducing endocytosis and inducing cellular PrP release. J Biol Chem 277:25457–25464. https://doi.org/10.1074/jbc.M203248200.
34. Prior M, Lehmann S, Sy MS, Molloy B, McMahon HE. 2007. Cyclodextrins inhibit replication of scrapie prion protein in cell culture. J Virol 81:11195–11207. https://doi.org/10.1128/JVI.02559-06.
35. Rouvinski A, Karniely S, Kounin M, Moussa S, Goldberg MD, Warburg G, Lyakhovetsky R, Papy-Garcia D, Kutzsche J, Korth C, Carlson GA, Godsave SF, Peters PJ, Luhr K, Kristensson K, Taraboulos A. 2014. Live imaging of prions reveals nascent PrPSc in cell-surface, raft-associated amyloid strings and webs. J Cell Biol 204:423–441. https://doi.org/10.1083/jcb.201308028.
36. White LP. 1958. Melanin: a naturally occurring cation exchange material. Nature 182:1427–1428. https://doi.org/10.1038/1821427a0.
37. Heiseke A, Aguib Y, Schatzl HM. 2010. Autophagy, prion infection and their mutual interactions. Curr Issues Mol Biol 12:87–97.
38. Marzo L, Marijanovic Z, Browman D, Chamoun Z, Caputo A, Zurzolo C. 2013. 4-hydroxytamoxifen leads to PrPSc clearance by conveying both PrPC and PrPSc to lysosomes independently of autophagy. J Cell Sci 126:1345–1354. https://doi.org/10.1242/jcs.114801.
39. Shim SY, Karri S, Law S, Schatzl HM, Gilch S. 2016. Prion infection impairs lysosomal degradation capacity by interfering with rab7 membrane attachment in neuronal cells. Sci Rep 6:21658. https://doi.org/10.1038/srep21658.
40. Thompson MJ, Borsenberger V, Louth JC, Judd KE, Chen B. 2009. Design, synthesis, and structure-activity relationship of indole-3-glyoxylamide libraries possessing highly potent activity in a cell line model of prion disease. J Med Chem 52:7503–7511. https://doi.org/10.1021/jm900920x.
41. Tagliavini F, Forloni G, Colombo L, Rossi G, Girola L, Canciani B, Angeretti N, Giampaolo L, Peressini E, Awan T, De Gioia L, Ragg E, Bugiani O, Salmona M. 2000. Tetracycline affects abnormal properties of synthetic PrP peptides and PrP(Sc) in vitro. J Mol Biol 300:1309–1322. https://doi.org/10.1006/jmbi.2000.3840.
42. Supattapone S, Piro JR, Rees JR. 2009. Complex polyamines: unique

prion disaggregating compounds. CNS Neurol Disord Drug Targets 8:323–328. https://doi.org/10.2174/187152709789541952.
43. Solano F. 2014. Melanins: skin pigments and much more—types, structural models, biological functions, and formation routes. New J Sci 2014:1–28.
44. Eleftherianos I, Revenis C. 2011. Role and importance of phenoloxidase in insect hemostasis. J Innate Immun 3:28–33. https://doi.org/10.1159/000321931.
45. Teruya K, Wakao M, Sato M, Hamanaka T, Nishizawa K, Funayama Y, Sakasegawa Y, Suda Y, Doh-ura K. 2015. Heparinase I-specific disaccharide unit of heparin is a key structure but insufficient for exerting anti-prion activity in prion-infected cells. Biochem Biophys Res Commun 460:989–995. https://doi.org/10.1016/j.bbrc.2015.03.139.
46. Kocisko DA, Vaillant A, Lee KS, Arnold KM, Bertholet N, Race RE, Olsen EA, Juteau JM, Caughey B. 2006. Potent antiscrapie activities of degenerate phosphorothioate oligonucleotides. Antimicrob Agents Chemother 50:1034–1044. https://doi.org/10.1128/AAC.50.3.1034-1044.2006.
47. Caughey B, Caughey WS, Kocisko DA, Lee KS, Silveira JR, Morrey JD. 2006. Prions and transmissible spongiform encephalopathy (TSE) chemotherapeutics: a common mechanism for anti-TSE compounds? Acc Chem Res 39:646–653. https://doi.org/10.1021/ar050068p.
48. Caughey B, Brown K, Raymond GJ, Katzenstein GE, Thresher W. 1994. Binding of the protease-sensitive form of PrP (prion protein) to sulfated glycosaminoglycan and Congo red [corrected]. J Virol 68:2135–2141.
49. Karpuj MV, Gelibter-Niv S, Tiran A, Rambold A, Tatzelt J, Nunziante M, Schatzl HM. 2011. Conditional modulation of membrane protein expression in cultured cells mediated by prion protein recognition of short phosphorothioate oligodeoxynucleotides. J Biol Chem 286:6911–6917. https://doi.org/10.1074/jbc.M110.194662.
50. Yokoyama T, Takeuchi A, Yamamoto M, Kitamoto T, Ironside JW, Morita M. 2011. Heparin enhances the cell-protein misfolding cyclic amplification efficiency of variant Creutzfeldt-Jakob disease. Neurosci Lett 498:119–123. https://doi.org/10.1016/j.neulet.2011.04.072.
51. Murayama Y, Yoshioka M, Masujin K, Okada H, Iwamaru Y, Imamura M, Matsuura Y, Fukuda S, Onoe S, Yokoyama T, Mohri S. 2010. Sulfated dextrans enhance in vitro amplification of bovine spongiform encephalopathy PrP(Sc) and enable ultrasensitive detection of bovine PrP(Sc). PLoS One 5:e13152. https://doi.org/10.1371/journal.pone.0013152.
52. Deleault NR, Lucassen RW, Supattapone S. 2003. RNA molecules stimulate prion protein conversion. Nature 425:717–720. https://doi.org/10.1038/nature01979.
53. Wakamatsu K, Takasaki A, Kagedal B, Kageshita T, Ito S. 2006. Determination of eumelanin in human urine. Pigment Cell Res 19:163–169. https://doi.org/10.1111/j.1600-0749.2006.00296.x.
54. Westerhof W, Pavel S, Kammeyer A, Beusenberg FD, Cormane R. 1987. Melanin-related metabolites as markers of the skin pigmentary system. J Investig Dermatol 89:78–81. https://doi.org/10.1111/1523-1747.ep12580422.
55. Ekelund MC, Carstam R, Hansson C, Rorsman H, Rosengren E. 1985. Urinary excretion of 5-S-cysteinyldopa and 6-hydroxy-5-methoxyindole-2-carboxylic acid: differences between pigmented and albino mice. Acta Derm Venereol 65:437–439.
56. Gudjohnsen SA, Atacho DA, Gesbert F, Raposo G, Hurbain I, Larue L, Steingrimsson E, Petersen PH. 2015. Meningeal melanocytes in the mouse: distribution and dependence on *Mitf*. Front Neuroanat 9:149. https://doi.org/10.3389/fnana.2015.00149.
57. Prota G. 1992. Neuromelanin, p 119–133. *In* Prota G (ed), Melanins and melanogenesis, Academic Press, San Diego, CA.
58. Zecca L, Zucca FA, Wilms H, Sulzer D. 2003. Neuromelanin of the substantia nigra: a neuronal black hole with protective and toxic characteristics. Trends Neurosci 26:578–580. https://doi.org/10.1016/j.tins.2003.08.009.
59. Fedorow H, Tribl F, Halliday G, Gerlach M, Riederer P, Double KL. 2005. Neuromelanin in human dopamine neurons: comparison with peripheral melanins and relevance to Parkinson's disease. Prog Neurobiol 75:109–124. https://doi.org/10.1016/j.pneurobio.2005.02.001.
60. Foley JM, Baxter D. 1958. On the nature of pigment granules in the cells of the locus coeruleus and substantia nigra. J Neuropathol Exp Neurol 17:586–598. https://doi.org/10.1097/00005072-195810000-00005.
61. Mann DM, Yates PO. 1974. Lipoprotein pigments—their relationship to ageing in the human nervous system. II. The melanin content of pigmented nerve cells. Brain 97:489–498.
62. Barden H, Levine S. 1983. Histochemical observations on rodent brain melanin. Brain Res Bull 10:847–851. https://doi.org/10.1016/0361-9230(83)90218-6.
63. Kim ST, Choi JH, Kim D, Hwang O. 2006. Increases in TH immunoreactivity, neuromelanin and degeneration in the substantia nigra of middle aged mice. Neurosci Lett 396:263–268. https://doi.org/10.1016/j.neulet.2005.11.053.
64. Shintaku M, Yutani C, Doh-ura K. 2006. Brain stem lesions in sporadic Creutzfeldt-Jakob disease: a histopathological and immunohistochemical study. Neuropathology 26:43–49. https://doi.org/10.1111/j.1440-1789.2006.00654.x.
65. Aronoff-Spencer E, Burns CS, Avdievich NI, Gerfen GJ, Peisach J, Antholine WE, Ball HL, Cohen FE, Prusiner SB, Millhauser GL. 2000. Identification of the Cu2+ binding sites in the N-terminal domain of the prion protein by EPR and CD spectroscopy. Biochemistry 39:13760–13771. https://doi.org/10.1021/bi001472t.
66. Burns CS, Aronoff-Spencer E, Dunham CM, Lario P, Avdievich NI, Antholine WE, Olmstead MM, Vrielink A, Gerfen GJ, Peisach J, Scott WG, Millhauser GL. 2002. Molecular features of the copper binding sites in the octarepeat domain of the prion protein. Biochemistry 41:3991–4001. https://doi.org/10.1021/bi011922x.
67. Qin K, Yang Y, Mastrangelo P, Westaway D. 2002. Mapping Cu(II) binding sites in prion proteins by diethyl pyrocarbonate modification and matrix-assisted laser desorption ionization-time of flight (MALDI-TOF) mass spectrometric footprinting. J Biol Chem 277:1981–1990. https://doi.org/10.1074/jbc.M108744200.
68. Walter ED, Stevens DJ, Visconte MP, Millhauser GL. 2007. The prion protein is a combined zinc and copper binding protein: Zn2+ alters the distribution of Cu2+ coordination modes. J Am Chem Soc 129:15440–15441. https://doi.org/10.1021/ja077146j.
69. Brazier MW, Davies P, Player E, Marken F, Viles JH, Brown DR. 2008. Manganese binding to the prion protein. J Biol Chem 283:12831–12839. https://doi.org/10.1074/jbc.M709820200.
70. Morillas M, Swietnicki W, Gambetti P, Surewicz WK. 1999. Membrane environment alters the conformational structure of the recombinant human prion protein. J Biol Chem 274:36859–36865. https://doi.org/10.1074/jbc.274.52.36859.
71. Wang F, Yin S, Wang X, Zha L, Sy MS, Ma J. 2010. Role of the highly conserved middle region of prion protein (PrP) in PrP-lipid interaction. Biochemistry 49:8169–8176. https://doi.org/10.1021/bi101146v.
72. Baron GS, Caughey B. 2003. Effect of glycosylphosphatidylinositol anchor-dependent and -independent prion protein association with model raft membranes on conversion to the protease-resistant isoform. J Biol Chem 278:14883–14892. https://doi.org/10.1074/jbc.M210840200.
73. Gabus C, Auxilien S, Pechoux C, Dormont D, Swietnicki W, Morillas M, Surewicz W, Nandi P, Darlix JL. 2001. The prion protein has DNA strand transfer properties similar to retroviral nucleocapsid protein. J Mol Biol 307:1011–1021. https://doi.org/10.1006/jmbi.2001.4544.
74. Weiss S, Proske D, Neumann M, Groschup MH, Kretzschmar HA, Famulok M, Winnacker EL. 1997. RNA aptamers specifically interact with the prion protein PrP. J Virol 71:8790–8797.
75. Sekiya S, Noda K, Nishikawa F, Yokoyama T, Kumar PK, Nishikawa S. 2006. Characterization and application of a novel RNA aptamer against the mouse prion protein. J Biochem 139:383–390. https://doi.org/10.1093/jb/mvj046.
76. Gomes MP, Millen TA, Ferreira PS, e Silva NL, Vieira TC, Almeida MS, Silva JL, Cordeiro Y. 2008. Prion protein complexed to N2a cellular RNAs through its N-terminal domain forms aggregates and is toxic to murine neuroblastoma cells. J Biol Chem 283:19616–19625. https://doi.org/10.1074/jbc.M802102200.
77. Pan T, Wong BS, Liu T, Li R, Petersen RB, Sy MS. 2002. Cell-surface prion protein interacts with glycosaminoglycans. Biochem J 368:81–90. https://doi.org/10.1042/bj20020773.
78. Warner RG, Hundt C, Weiss S, Turnbull JE. 2002. Identification of the heparan sulfate binding sites in the cellular prion protein. J Biol Chem 277:18421–18430. https://doi.org/10.1074/jbc.M110406200.
79. Taubner LM, Bienkiewicz EA, Copie V, Caughey B. 2010. Structure of the flexible amino-terminal domain of prion protein bound to a sulfated glycan. J Mol Biol 395:475–490. https://doi.org/10.1016/j.jmb.2009.10.075.
80. Lee KS, Raymond LD, Schoen B, Raymond GJ, Kett L, Moore RA, Johnson LM, Taubner L, Speare JO, Onwubiko HA, Baron GS, Caughey WS, Caughey B. 2007. Hemin interactions and alterations of the subcellular

localization of prion protein. J Biol Chem 282:36525–36533. https://doi.org/10.1074/jbc.M705620200.
81. Parkyn CJ, Vermeulen EG, Mootoosamy RC, Sunyach C, Jacobsen C, Oxvig C, Moestrup S, Liu Q, Bu G, Jen A, Morris RJ. 2008. LRP1 controls biosynthetic and endocytic trafficking of neuronal prion protein. J Cell Sci 121:773–783. https://doi.org/10.1242/jcs.021816.
82. Solforosi L, Bellon A, Schaller M, Cruite JT, Abalos GC, Williamson RA. 2007. Toward molecular dissection of PrPC-PrPSc interactions. J Biol Chem 282:7465–7471.
83. Resenberger UK, Harmeier A, Woerner AC, Goodman JL, Muller V, Krishnan R, Vabulas RM, Kretzschmar HA, Lindquist S, Hartl FU, Multhaup G, Winklhofer KF, Tatzelt J. 2011. The cellular prion protein mediates neurotoxic signalling of beta-sheet-rich conformers independent of prion replication. EMBO J 30:2057–2070. https://doi.org/10.1038/emboj.2011.86.
84. Chen S, Yadav SP, Surewicz WK. 2010. Interaction between human prion protein and amyloid-beta (Abeta) oligomers: role of N-terminal residues. J Biol Chem 285:26377–26383. https://doi.org/10.1074/jbc.M110.145516.
85. Beland M, Roucou X. 2012. The prion protein unstructured N-terminal region is a broad-spectrum molecular sensor with diverse and contrasting potential functions. J Neurochem 120:853–868. https://doi.org/10.1111/j.1471-4159.2011.07613.x.
86. Oliveira-Martins JB, Yusa S, Calella AM, Bridel C, Baumann F, Dametto P, Aguzzi A. 2010. Unexpected tolerance of alpha-cleavage of the prion protein to sequence variations. PLoS One 5:e9107. https://doi.org/10.1371/journal.pone.0009107.
87. Turnbaugh JA, Unterberger U, Saa P, Massignan T, Fluharty BR, Bowman FP, Miller MB, Supattapone S, Biasini E, Harris DA. 2012. The N-terminal, polybasic region of PrP(C) dictates the efficiency of prion propagation by binding to PrP(Sc). J Neurosci 32:8817–8830. https://doi.org/10.1523/JNEUROSCI.1103-12.2012.
88. Martinez J, Sanchez R, Castellanos M, Makarava N, Aguzzi A, Baskakov IV, Gasset M. 2015. PrP charge structure encodes interdomain interactions. Sci Rep 5:13623. https://doi.org/10.1038/srep13623.
89. Guillot-Sestier MV, Sunyach C, Druon C, Scarzello S, Checler F. 2009. The alpha-secretase-derived N-terminal product of cellular prion, N1, displays neuroprotective function in vitro and in vivo. J Biol Chem 284:35973–35986. https://doi.org/10.1074/jbc.M109.051086.
90. Turnbaugh JA, Westergard L, Unterberger U, Biasini E, Harris DA. 2011. The N-terminal, polybasic region is critical for prion protein neuroprotective activity. PLoS One 6:e25675. https://doi.org/10.1371/journal.pone.0025675.
91. Li C, Hou J, Gu J, Han Q, Guan Y, Zhang Y. 2015. Synthesis and thermal gelation of hydroxypropyl chitin. RSC Adv 5:39677–39685. https://doi.org/10.1039/C5RA03967C.
92. Montefiori DC, Zhou JY. 1991. Selective antiviral activity of synthetic soluble L-tyrosine and L-dopa melanins against human immunodeficiency virus in vitro. Antiviral Res 15:11–25. https://doi.org/10.1016/0166-3542(91)90037-R.
93. Kawasaki Y, Kawagoe K, Chen CJ, Teruya K, Sakasegawa Y, Doh-ura K. 2007. Orally administered amyloidophilic compound is effective in prolonging the incubation periods of animals cerebrally infected with prion diseases in a prion strain-dependent manner. J Virol 81:12889–12898. https://doi.org/10.1128/JVI.01563-07.
94. Ishikawa K, Kudo Y, Nishida N, Suemoto T, Sawada T, Iwaki T, Doh-ura K. 2006. Styrylbenzoazole derivatives for imaging of prion plaques and treatment of transmissible spongiform encephalopathies. J Neurochem 99:198–205. https://doi.org/10.1111/j.1471-4159.2006.04035.x.
95. Doh-ura K, Iwaki T, Caughey B. 2000. Lysosomotropic agents and cysteine protease inhibitors inhibit scrapie-associated prion protein accumulation. J Virol 74:4894–4897. https://doi.org/10.1128/JVI.74.10.4894-4897.2000.
96. Nishizawa K, Oguma A, Kawata M, Sakasegawa Y, Teruya K, Doh-ura K. 2014. Efficacy and mechanism of a glycoside compound inhibiting abnormal prion protein formation in prion-infected cells: implications of interferon and phosphodiesterase 4D-interacting protein. J Virol 88:4083–4099. https://doi.org/10.1128/JVI.03775-13.
97. Teruya K, Nishizawa K, Doh-ura K. 2010. Semisynthesis of a protein with cholesterol at the C-terminal, targeted to the cell membrane of live cells. Protein J 29:493–500. https://doi.org/10.1007/s10930-010-9278-9.
98. Hamanaka T, Nishizawa K, Sakasegawa Y, Teruya K, Doh-ura K. 2015. Structure-activity analysis and antiprion mechanism of isoprenoid compounds. Virology 486:63–70. https://doi.org/10.1016/j.virol.2015.09.002.
99. Iwamaru Y, Shimizu Y, Imamura M, Murayama Y, Endo R, Tagawa Y, Ushiki-Kaku Y, Takenouchi T, Kitani H, Mohri S, Yokoyama T, Okada H. 2008. Lactoferrin induces cell surface retention of prion protein and inhibits prion accumulation. J Neurochem 107:636–646. https://doi.org/10.1111/j.1471-4159.2008.05628.x.
100. Kuwahara C, Takeuchi AM, Nishimura T, Haraguchi K, Kubosaki A, Matsumoto Y, Saeki K, Matsumoto Y, Yokoyama T, Itohara S, Onodera T. 1999. Prions prevent neuronal cell-line death. Nature 400:225–226. https://doi.org/10.1038/22241.
101. Hirobe T. 2011. How are proliferation and differentiation of melanocytes regulated? Pigment Cell Melanoma Res 24:462–478. https://doi.org/10.1111/j.1755-148X.2011.00845.x.
102. Race RE, Priola SA, Bessen RA, Ernst D, Dockter J, Rall GF, Mucke L, Chesebro B, Oldstone MB. 1995. Neuron-specific expression of a hamster prion protein minigene in transgenic mice induces susceptibility to hamster scrapie agent. Neuron 15:1183–1191. https://doi.org/10.1016/0896-6273(95)90105-1.
103. Teruya K, Oguma A, Nishizawa K, Kawata M, Sakasegawa Y, Kamitakahara H, Doh-ura K. 2016. A single subcutaneous injection of cellulose ethers administered long before infection confers sustained protection against prion diseases in rodents. PLoS Pathog 12:e1006045. https://doi.org/10.1371/journal.ppat.1006045.